



Nonlinear Forced Vibration of Cantilevered Pipes Conveying Fluid

Zhi-Yuan Liu^{1,2} Lin Wang^{1,2*} Xi-Ping Sun³

⁽¹⁾Department of Mechanics, Huazhong University of Science and Technology, Wuhan 430074, China)

⁽²⁾Hubei Key Laboratory for Engineering Structural Analysis and Safety Assessment, Wuhan 430074, China)

⁽³⁾Tianjin Research Institute Water Transport Engineering, M.O.T., Test Detection Center of Water Transport Engineering, Tianjin 300456, China)

Received 20 September 2017; revision received 5 December 2017; Accepted 19 January 2018;
published online 7 March 2018

© The Chinese Society of Theoretical and Applied Mechanics and Technology 2018

ABSTRACT The nonlinear forced vibrations of a cantilevered pipe conveying fluid under base excitations are explored by means of the full nonlinear equation of motion, and the fourth-order Runge–Kutta integration algorithm is used as a numerical tool to solve the discretized equations. The self-excited vibration is briefly discussed first, focusing on the effect of flow velocity on the stability and post-flutter dynamical behavior of the pipe system with parameters close to those in previous experiments. Then, the nonlinear forced vibrations are examined using several concrete examples by means of frequency response diagrams and phase-plane plots. It shows that, at low flow velocity, the resonant amplitude near the first-mode natural frequency is larger than its counterpart near the second-mode natural frequency. The second-mode frequency response curve clearly displays a softening-type behavior with hysteresis phenomenon, while the first-mode frequency response curve almost maintains its neutrality. At moderate flow velocity, interestingly, the first-mode resonance response diminishes and the hysteresis phenomenon of the second-mode response disappears. At high flow velocity beyond the flutter threshold, the frequency response curve would exhibit a quenching-like behavior. When the excitation frequency is increased through the quenching point, the response of the pipe may shift from quasiperiodic to periodic. The results obtained in the present work highlight the dramatic influence of internal fluid flow on the nonlinear forced vibrations of slender pipes.

KEY WORDS Pipe conveying fluid, Base excitation, Nonlinear dynamics, Primary resonance, Superharmonic resonance, Forced vibration

1. Introduction

Among various dynamical systems, perhaps the column subjected to compressive loading, the rotating shaft, the van der Pol's oscillator, and Lorenz equations are the most famous examples of model problems for the study of stability and nonlinear dynamics. By referring to recent work, it is interesting to note that the pipe conveying fluid has established itself as a generic paradigm of a kaleidoscope of interesting dynamical behavior [1–4]. Indeed, the dynamics of pipes conveying fluid has been investigated extensively by researchers around the world. In the research field of dynamics of pipes conveying fluid, Paidoussis has dedicated his famous book on various aspects of the problem of a pipe conveying

* Corresponding author. E-mail:wanglindds@hust.edu.cn

fluid [3]. The interested reader is referred to his book for a comprehensive introduction to the dynamics of pipes conveying fluid and the possible applications of the knowledge gained from studying this dynamical problem.

As the dynamic systems of cantilevered and supported (straight) pipes conveying fluid are fundamentally different, i.e., the former is non-conservative, but the latter is conservative in the absence of dissipation, they have been treated separately. For fluid-conveying pipes with both ends supported, the expected form of instability at a certain critical flow velocity is divergence (buckling) [5–8], similar to that of a column subjected to compressive loading. After buckling instability, the post-buckling amplitude of the supported pipe with increasing flow velocity would increase [9]. Nevertheless, no other types of instability could be observed in such a pipe system [10]. For a cantilevered pipe conveying fluid, however, flutter rather than buckling instability occurs at a critical flow velocity, at which a Hopf bifurcation occurs, and beyond which the pipe undergoes periodic motions (limit cycle motions) for higher flow velocities [11]. The post-flutter response of the cantilevered pipe may be either two-dimensional (2D) or three-dimensional (3D), mainly depending on the mass ratio parameter and flow velocity [12–14].

When a clamped-free straight pipe conveying fluid is additionally subjected to a spring, a mass, or motion constraints at a point along its length, the self-excited vibration becomes much more complicated than that of a plain pipe. For instance, the occurrence of double degeneracy is possible in a slender, vertically ‘standing’ cantilever conveying fluid with an intermediate linear spring support [15, 16]; pitchfork and period-doubling bifurcations may occur in a vertically ‘hanging’ cantilever conveying fluid when an additional cubic spring is placed somewhere along its length [17–22]; chaotic motions and sticking phenomenon can be generated in a cantilevered pipe conveying fluid with loose constraints added [23, 24]; non-planar motions can be induced when a cantilevered pipe conveying fluid is modified by adding a lumped mass at the tip end [25–28]. Therefore, extremely rich dynamics can be observed in the slightly modified variants of the basic system.

Several researchers studied the dynamics of cantilevered pipes conveying harmonically perturbed flow. In the presence of pulsatile flow velocity, the so-called parametric resonances can occur under certain conditions. Bajaj [13] conducted a complete bifurcation analysis of the principle primary resonance in the vicinity of flutter boundaries. It was found that for a cantilevered pipe conveying pulsatile flow, in most cases, the Hopf bifurcation is suppressed and the dynamics is dominated by the parametric resonance. Semler and Paidoussis [29] extended Bajaj’s work by providing numerical solutions of the full nonlinear equations and some experimental results. Recently, Folley and Bajaj [30] extended Bajaj’s work [13] to study the 3D motions of a pipe conveying pulsatile flow with emphasis on the principal parametric resonance, showing some complex dynamical behavior.

In the above-mentioned literature, only self-excited oscillations were considered. Recently, a few studies have dealt with the forced vibrations of cantilevered pipes conveying fluid [31–33]. In some engineering cases, the base (clamped end) of the pipe is movable. For example, in ocean engineering, the upstream end of a marine riser conveying fluid is usually attached to a rolling ship. In this case, the clamped end of the riser moves, and the riser is subjected to a base excitation. For a fluid-conveying pipe in the presence of base excitations, as expected, both self-excited and forced oscillations would occur when the flow velocity becomes high. Furuya et al. [32] investigated the stability of a cantilevered pipe conveying fluid with an end mass in the case of a base excitation at the clamped end, for flow velocities slightly higher than the critical value. They found that non-planar vibrations could be reduced to planar ones when excitation frequencies are nearly equal to the resonant frequency of the basic system of pipes conveying fluid. This finding was further verified using experimental results. More recently, a numerical analysis was conducted on the effect of a small amplitude periodic base excitation on the 2D and 3D oscillations of a cantilevered pipe conveying fluid over a wide range of flow velocities by Chang and Modarres-Sadeghi [33], who utilized the 3D version of nonlinear equations and analyzed the dynamic response in the case of a pipe with excitation frequencies near the second- or third-mode resonant frequency. It was found that, in the presence of base excitations with a proper frequency and relatively small amplitudes, it is possible to control the pipe’s non-planar motion and limit it to a planar motion in a pre-defined direction.

For cantilevered pipes conveying fluid, therefore, it is found that the literature on the topic of self-excited vibrations is very extensive, while the work on forced vibrations is relatively limited. The

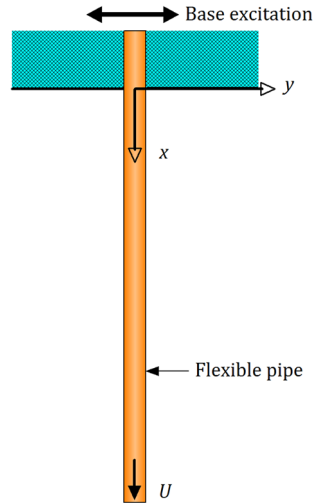


Fig. 1. Schematic of a cantilever conveying fluid subjected to a base excitation

studies by Furuya et al. [32] and Chang and Modarres-Sadeghi [33] were mainly concerned with the 3D oscillations of cantilevered pipe systems under base excitations. In the present work, a comprehensive study will be conducted on the planar oscillations of a cantilevered pipe conveying fluid over a wide range of flow velocities in the presence of a base excitation. The oscillations of the pipe are supposed to be planar by using a thin steel strip embedded in the pipe. All system parameters are chosen the same as those of the self-excited system of a pipe experimentally examined by Paidoussis and Semler [24]. The self-excited vibration of cantilevered pipes with no base excitation will be briefly discussed first. Then, the dynamic responses of the pipe subjected to a periodic base excitation are explored for various flow velocities, excitation frequencies, and excitation amplitudes. The main goal is to find the underlying correlation between the pipe's oscillations and the base excitation.

2. Modeling of the Pipe System

2.1. Equation of Motion

The dynamical system under consideration consists of a tubular, vertical, cantilevered beam of length L , flexural rigidity EI , and mass per unit length m . The upstream end of the pipe is clamped and the downstream end is free. The fluid flowing in the cantilevered pipe is of mass M per unit length, flowing with a steady flow velocity U . In order to keep the dynamics as simple as possible for analytical modeling, the oscillation is restricted to a plane by embedding a thin metal plate all along the length of the pipe. As shown in Fig. 1, the slender pipe is assumed to lie initially along the x -axis and oscillate in the (x, y) plane with motion $W(s, t)$, s being the curvilinear coordinate, and t the time. The pipe is subjected to a transverse base excitation in the y -axis direction in the form of $D_0 \sin(\Omega t)$, with D_0 and Ω being the amplitude and frequency of the base excitation, respectively.

According to the work by Semler et al. [34], if the base excitation is absent, the nonlinear equation of motion can be derived via the Hamiltonian method and may be finally written in dimensionless form as follows:

$$\begin{aligned}
 & [w''''(1 + w'^2) + 4w'w''w''' + \eta''^3] + \ddot{w} + 2u\sqrt{\beta}\dot{w}'(1 + w'^2) + \sigma\dot{w} \\
 & + \gamma \left(1 + \frac{1}{2}w'^2 \right) w' + \left[u^2(1 + w'^2) - \gamma(1 - \xi) \left(1 + \frac{3}{2}w'^2 \right) \right] w'' + w' \int_0^\xi (\dot{w}'^2 + w'\ddot{w}') d\xi \\
 & - w'' \left[\int_\xi^1 \int_0^\xi (\dot{w}'^2 + w'\ddot{w}') d\xi d\xi + \int_\xi^1 (2u\sqrt{\beta}w'\dot{w}' + u^2w'w'') d\xi \right] = 0
 \end{aligned} \quad (1)$$

In Eq. (1), the dot denotes the derivative with respect to the dimensionless time τ ; the prime denotes the derivative with respect to the dimensionless curvilinear coordinate along the inextensible

centerline of the pipe, ξ ; $w(\xi, \tau)$ represents the lateral displacement of the pipe, u the dimensionless flow velocity, γ a dimensionless gravity parameter, β the mass ratio, and σ a damping coefficient. All the dimensionless quantities appearing in Eq. (1) are related to the dimensional parameters via

$$\begin{aligned} \xi &= \frac{s}{L}, \quad w = \frac{W}{L}, \quad \tau = \left(\frac{EI}{m+M} \right)^{1/2} \frac{t}{L^2}, \quad u = \left(\frac{M}{EI} \right)^{1/2} UL, \quad \beta = \frac{M}{M+m}, \\ \gamma &= \frac{m+M}{EI} L^3 g, \quad \sigma = \frac{cL^2}{[(m+M)EI]^{1/2}} \end{aligned} \quad (2)$$

where g is the acceleration due to gravity and c is the viscous damping coefficient resulting from the surrounding medium.

The total transverse displacement of the pipe, $w(\xi, \tau)$, can be expressed as the sum of the displacement of the pipe relative to the support (i.e., $w^*(\xi, \tau)$) and the displacement of the support itself. Thus, Eq. (1) can be rewritten as

$$\begin{aligned} & [w''''(1+w'^2) + 4w'w''w''' + \eta''^3] + \ddot{w} + 2u\sqrt{\beta}\dot{w}'(1+w'^2) + \sigma\dot{w} \\ & + \gamma \left(1 + \frac{1}{2}w'^2 \right) w' + \left[u^2(1+w'^2) - \gamma(1-\xi) \left(1 + \frac{3}{2}w'^2 \right) \right] w'' + w' \int_0^\xi (\dot{w}'^2 + w'\ddot{w}') d\xi \\ & - w'' \left[\int_\xi^1 \int_0^\xi (\dot{w}'^2 + w'\ddot{w}') d\xi d\xi + \int_\xi^1 (2u\sqrt{\beta}w'\dot{w}' + u^2w'w'') d\xi \right] \\ & - d_0\bar{\Omega}^2 \sin(\bar{\Omega}\tau) + \sigma d_0\bar{\Omega} \cos(\bar{\Omega}\tau) = 0 \end{aligned} \quad (3)$$

with

$$d_0 = \frac{D_0}{L}, \quad \bar{\Omega} = \Omega \sqrt{\frac{(m+M)L^4}{EI}} \quad (4)$$

where the superscript asterisk notation for relative displacement is dropped for brevity. For the pipe system shown in Fig. 1, the boundary conditions to be satisfied are given by $w(0, \tau) = w'(0, \tau) = w''(1, \tau) = w'''(1, \tau) = 0$.

It is noted that the nonlinear inertial terms appearing in Eq. (3) can be converted to equivalent stiffness and velocity-dependent terms via a perturbation technique [34]. Therefore, after some straightforward algebra, Eq. (3) can be rewritten as

$$\begin{aligned} & w'''' + \ddot{w} + 2u\sqrt{\beta}\dot{w}' + [u^2 - \gamma(1-\xi)]w'' + \gamma w' + \sigma\dot{w} + N(w) \\ & - d_0\bar{\Omega}^2 \sin(\bar{\Omega}\tau) + \sigma d_0\bar{\Omega} \cos(\bar{\Omega}\tau) = 0 \end{aligned} \quad (5)$$

in which the nonlinear term $N(w)$ is given by

$$\begin{aligned} N(w) &= 2u\sqrt{\beta}\dot{w}'w'^2 + w'' \left[u^2 - \frac{3}{2}\gamma(1-\xi) \right] w'^2 - \frac{1}{2}\gamma w'^3 + 3w'w''w''' + w'^3 \\ &+ w' \int_0^\xi \left\{ \dot{w}'^2 - 2u\sqrt{\beta}w'\dot{w}'' - w'w''''[u^2 - \gamma(1-\xi)] + w''w'''' \right\} d\xi \\ &- w'' \int_\xi^1 \int_0^\xi \left[\dot{w}'^2 - 2u\sqrt{\beta}w'\dot{w}'' - w'w''''[u^2 - \gamma(1-\xi)] + w''w'''' \right] d\xi d\xi \\ &- w'' \int_\xi^1 \left(-\gamma w'^2 + 2u\sqrt{\beta}w'\dot{w}' + u^2w'w'' + w''w'''' \right) d\xi \end{aligned} \quad (6)$$

As suggested by Paidoussis et al. [19], for visco hysteretic damping characteristics of the pipe, a modal damping representation is suitable. In this way, for the r th mode, the damping term in Eq. (5) can be modified by using the following expression:

$$\sigma_r \dot{w} = \frac{\delta_r \omega_{0r}}{\pi} \dot{w} \quad (7)$$

where ω_{0r} are the zero-flow dimensionless eigenfrequencies of the pipe; and δ_r can be measured for small r and linearly extrapolated for large r when required.

2.2. Method of Solution

The nonlinear equation of motion of the vertical cantilever conveying fluid under base excitations will be discretized by means of the Galerkin's technique, with the eigenfunctions of a cantilevered beam, $\varphi_r(\xi)$, being used as a suitable set of base functions, as well as the corresponding generalized coordinates $q_r(\tau)$. Thus, we let

$$w(\xi, \tau) = \sum_{r=1}^{\infty} \varphi_r(\xi) q_r(\tau) \quad (8)$$

where $\varphi_r(\xi) = \cosh \lambda_r \xi - \cos \lambda_r \xi - \theta_r (\sinh \lambda_r \xi - \sin \lambda_r \xi)$, with $\theta_r = (\sinh \lambda_r - \sin \lambda_r) / (\cosh \lambda_r + \cos \lambda_r)$.

The substitution of expression (8) into (5), followed by multiplication by $\varphi_r(\xi)$ and integration over the domain $[0,1]$, leads to

$$\ddot{\mathbf{q}} + \mathbf{C}\dot{\mathbf{q}} + \mathbf{K}\mathbf{q} + \mathbf{f}(\mathbf{q}, \dot{\mathbf{q}}) = \mathbf{0} \quad (9)$$

where \mathbf{q} is the generalized displacement vector; \mathbf{C} and \mathbf{K} represent the elements of damping and stiffness matrices, respectively; and \mathbf{f} denotes the nonlinear term. The elements of the coefficient matrices \mathbf{C} and \mathbf{K} can be numerically computed from the integrals of the eigenfunctions $\varphi_i(\xi)$. Once the generalized coordinates $q_r(\tau)$ have been calculated based on Eq. (9), the lateral deflection of the pipe can be expressed using Eq. (8) with a suitably high value of $r = N$.

Before leaving this section, it should be mentioned that Eq. (9) may be further rewritten in first-order form, the solutions of which can be obtained by using a fourth-order Runge–Kutta integration algorithm. It should be mentioned that, in our numerical procedure, the matrix transformation method [35] has been proposed to calculate the nonlinear term \mathbf{f} of Eq. (9). In the following calculations, the initial conditions for Eq. (9) are chosen as: $q_1(0) = 0.002$, $q_i(0) = 0$ for $i \geq 2$, and $\dot{q}_i(0) = 0$ ($i = 1, 2, \dots, N$). The numerical results will be mainly presented in the form of bifurcation diagrams, phase portraits, frequency response diagrams, and oscillating shape plots, as discussed below.

3. Results

In this section, the nonlinear forced vibration of a vertically hanging cantilever conveying fluid under a base excitation is investigated when the flow velocity, u , is varied to show the rich dynamics of the system. For that purpose, calculations with the same parameters as those utilized by Paidoussis and Semler [24] are used: i.e., $\beta = 0.213$, $\gamma = 26.75$, $\delta_1 = 0.028$, $\delta_2 = 0.081$, $\delta_3 = 0.144$, $\delta_4 = 0.200$, and $\delta_5 = 0.260$. These dimensionless system parameters correspond to the experimentally measured values for a vertically hanging pipe with no base excitation.

Although the self-excited vibrational behavior of a cantilever conveying fluid without base excitation has been described elsewhere [3, 24], a few words on the self-excited vibrations will nevertheless be useful for our further analysis on the forced vibrations. Thus, the self-excited vibrations of the dynamical system will be revisited first to verify the reliability and accuracy of our numerical procedure. Then, the nonlinear forced vibrations of the pipe system such as the primary and superharmonic resonances will be studied separately.

3.1. Self-excited Vibrations of the Cantilever Conveying Fluid

The linear dynamical behavior of the cantilevered pipe conveying fluid may be clearly shown in the form of Argand diagram. Typical results using $N = 4$ are plotted in Fig. 2, where $\text{Re}(\omega)$ is the oscillation frequency, while $\text{Im}(\omega)$ is related to the damping, with the damping ratio being $\zeta = \text{Im}(\omega)/\text{Re}(\omega)$. It is seen that for the flow velocity varied in the range $0 \leq u \leq 7$, the internal flow induces positive damping in the lowest four modes of the system, i.e., $\zeta = \text{Im}(\omega)/\text{Re}(\omega) > 0$. With increasing u , $\text{Im}(\omega)$ in the first, third, and fourth modes becomes larger, at least up to $u = 10$. For higher u , however, $\text{Im}(\omega)$ in the second mode of the system eventually becomes negative. As can be observed in Fig. 2, a flutter instability (Hopf bifurcation) occurs at $u = u_{\text{cr}} \simeq 8.54$.

The lowest three oscillation frequencies of the pipe system for several values of flow velocity are summarized in Table 1. For $u = 7.4, 8.5, 8.6$ or 9 , it is seen that the first-mode frequency is zero. However, all the values of $\text{Im}(\omega)$ keep positive (Fig. 2), indicating that the first mode is stable.

As we know, flutter instability is often generated via a Hopf bifurcation and implies the generation of a limit cycle. The prediction of post-flutter behaviors of the pipe requires a nonlinear analysis.

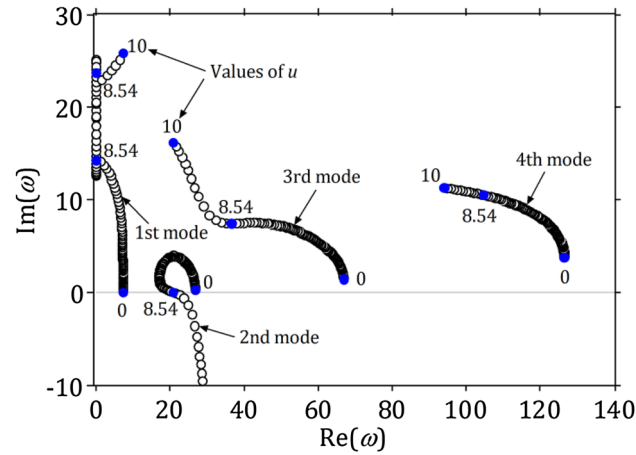


Fig. 2. Dimensionless complex frequency of the four lowest modes of the linear system as a function of the dimensionless flow velocity, for $\beta = 0.213$ and $\gamma = 26.75$

Table 1. Lowest three oscillation frequencies of the fluid-conveying pipe for several values of flow velocity

Flow velocity (u)	Dimensionless oscillation frequency ($\text{Re}(\omega)$)		
	First mode	Second mode	Third mode
0.00	7.3471	26.7506	66.8477
0.25	7.3456	26.7334	66.8216
1.00	7.3295	26.5023	66.4905
2.00	7.2840	25.7662	65.4547
7.30	1.4162	17.1698	46.8712
7.40	0	17.2569	46.2096
8.50	0	20.8146	36.6234
8.60	0	21.5783	35.3391
9.00	0	28.9544	25.9158
10.0	8.4058	29.6116	20.0318

To quantitatively show the self-excited oscillations of the pipe in the post-flutter regime, a bifurcation diagram is presented in Fig. 3a based on a four-mode approximation (i.e., $N = 4$). Two phase portraits for $u = 8.0$ and 10.0 are plotted in Fig. 3b. By inspecting Fig. 3a, b, it is clear that the trajectory of the pipe is toward a fixed point for $u = 8.0$ while the pipe undergoes a symmetric limit cycle motion for $u = 10.0$. All the results of Fig. 3 regarding the nonlinear responses of a cantilevered pipe conveying fluid are consistent with previous conclusions [3].

To further check our numerical scheme, we consider another example of a fluid-conveying cantilever subjected to a cubic spring at $\xi = \xi_b = 0.65$ with the system parameters given by: $\gamma = 26.75$, $\beta = 0.213$, $k_3 = 10^5$, and $N = 3$ [24], where k_3 represents the dimensionless stiffness of the additional cubic spring. The comparison between our results and those of [24] is given in Fig. 4. It is seen that in the range of $7.5 < u < 11$, our result of bifurcation diagram shown in Fig. 4b agrees well with that of Fig. 4a reported by Paidoussis and Semler [24], thus demonstrating that our numerical scheme is reliable.

3.2. Forced Vibrations of the Cantilever Conveying Fluid Under a Base Excitation

3.2.1. Study of Convergence

As mentioned in the foregoing, the original partial differential equation (PDE) has been discretized using the Galerkin technique. The truncation of the Galerkin technique needs a sufficient number of comparison functions. Thus, the selected value of N must be suitable for actually predicting the dynamical behavior of the pipe system. Generally, the solutions of Eq. (9) need to be found for increasing values of N till the solutions do not change any more. A complete convergence study for the self-excited vibrations of the pipe system has been performed by Paidoussis and Semler [24]. For nonlinear

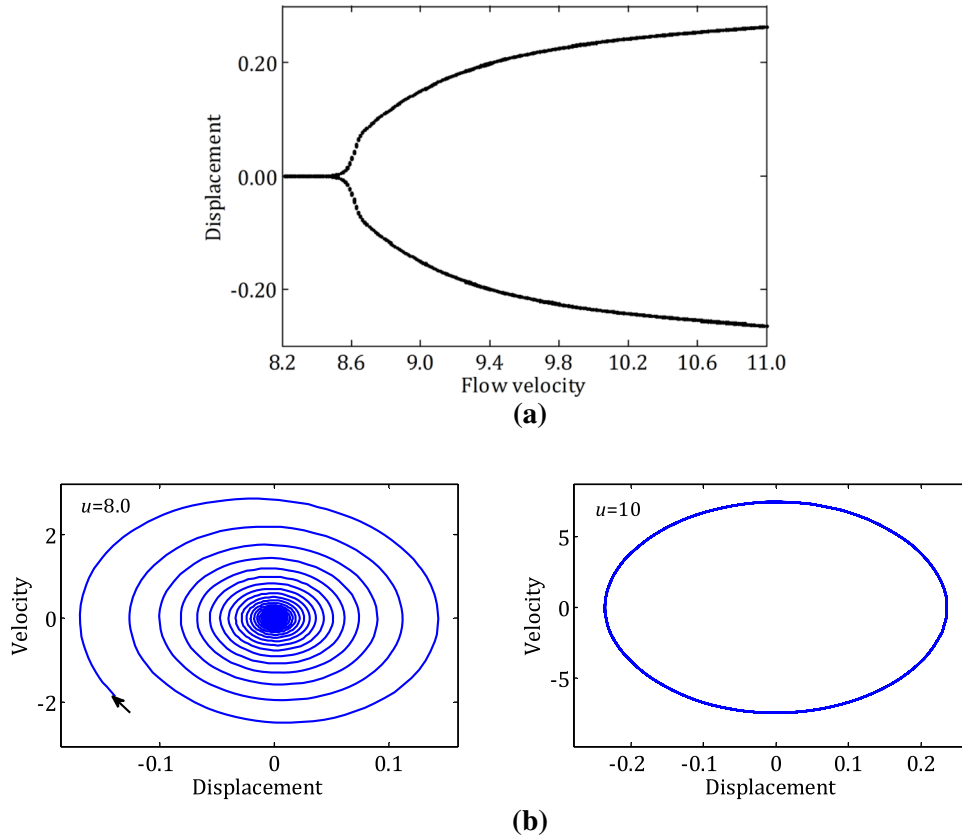


Fig. 3. **a** Bifurcation diagram of the dimensionless pipe-end displacement ($w(1, \tau)$) versus u and **b** two corresponding phase portraits for the cantilevered pipe system, for $\beta = 0.213$ and $\gamma = 26.75$

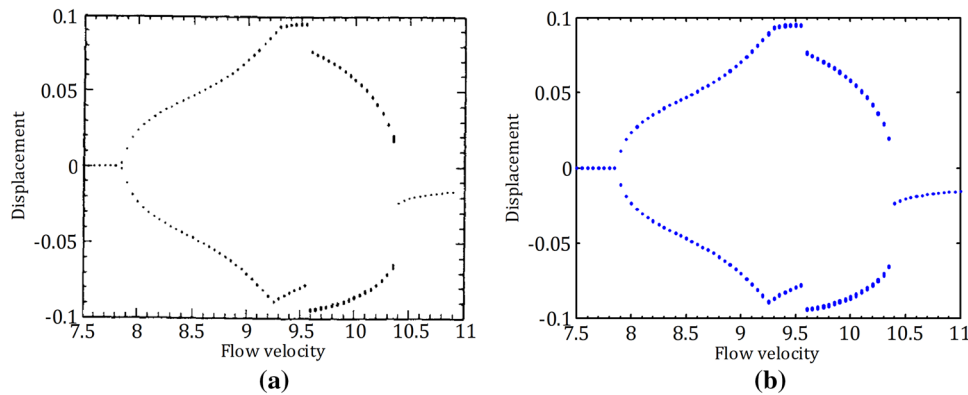


Fig. 4. Bifurcation diagrams for a fluid-conveying cantilever with a cubic spring when the flow velocity is varied, for $\gamma = 26.75$, $\beta = 0.213$, $k_3 = 10^5$, $\xi_b = 0.65$, and $N = 3$: **a** the results given in [24], **b** the present results

problems, they showed that for $u < 10$ approximately, the $N = 4$ modeling is a good approximation. This is why we have chosen $N = 4$ for calculations in Sect. 3.1.

In the current work, the fluid-conveying pipe is additionally subjected to a base excitation. It is then required to examine the reliability of the $N = 4$ modeling for the prediction of forced vibrations. In order to achieve proper convergence, the results of frequency response diagrams for $N = 2, 4$, and 5 are shown in Figs. 5, 6, and 7, for $u = 0.25$ and $\mu = 0.01$. In these three figures, the oscillation amplitudes of the tip-end displacements of the pipe were recorded for various dimensionless excitation

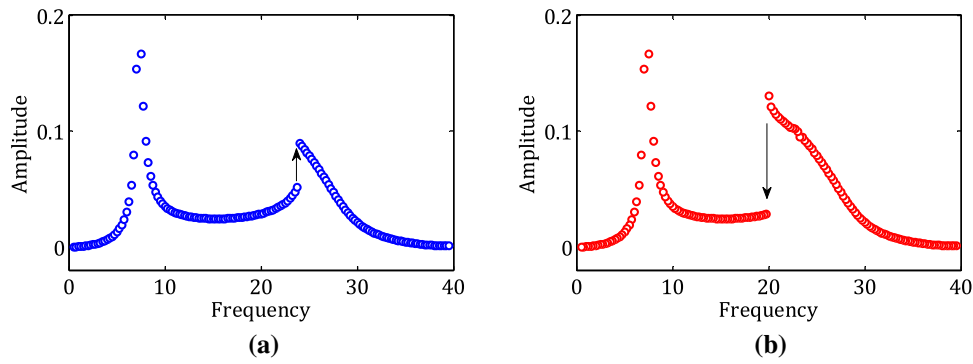


Fig. 5. Frequency response curves in the sense of primary resonances calculated using a two-mode approximation, for $u = 0.25$, $\mu = 0.01$, $\gamma = 26.75$, and $\beta = 0.213$; **a** the results for excitation frequencies being increased, and **b** the results for excitation frequencies being decreased

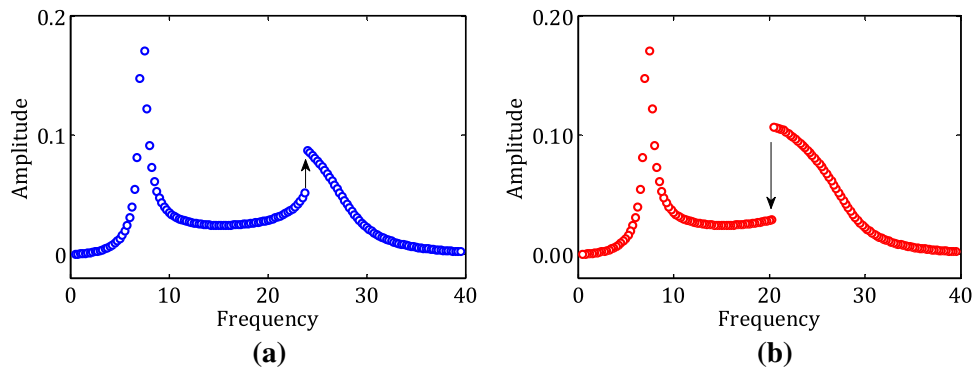


Fig. 6. Frequency response curves in the sense of primary resonances calculated using a four-mode approximation, for $u = 0.25$, $\mu = 0.01$, $\gamma = 26.75$, and $\beta = 0.213$; **a** the results for excitation frequencies being increased, and **b** the results for excitation frequencies being decreased

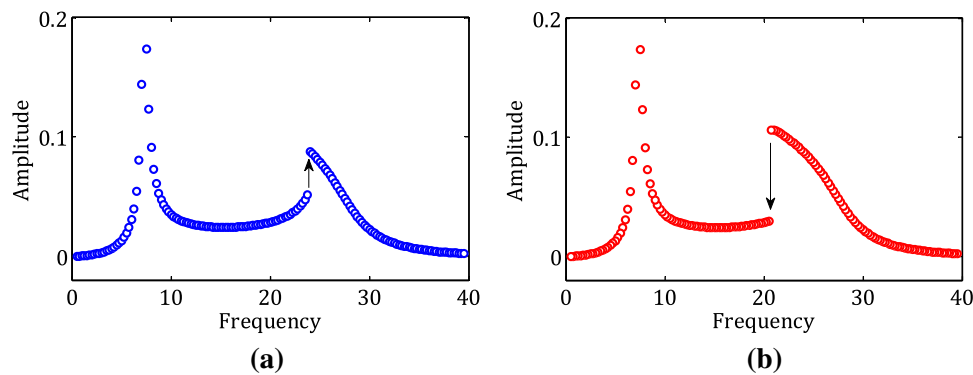


Fig. 7. Frequency response curves in the sense of primary resonances calculated using a five-mode approximation, for $u = 0.25$, $\mu = 0.01$, $\gamma = 26.75$, and $\beta = 0.213$; **a** the results for excitation frequencies being increased, and **b** the results for excitation frequencies being decreased

frequencies. In each figure, the frequency of the excitation is slowly varied up or down through the frequency domain of $[0, 40]$. It is immediately seen that the frequency response curves for $N = 2$ are similar to the counterparts shown for $N = 4$ or 5 . Particularly, the results shown in Fig. 6 for $N = 4$ are almost identical to that shown in Fig. 7 for $N = 5$, indicating that the approximation of the $N = 4$ modeling can accurately predict the nonlinear responses of the pipe under base excitation, at least up

to $\bar{\Omega} = 40$. For higher excitation frequencies (e.g., $\bar{\Omega} = 200$), however, higher-mode approximation may be required.

3.2.2. Dynamical Behavior of the Pipe Under a Base Excitation for Low Flow Velocity

It is instructive to examine the possible responses of the cantilever for very low flow velocities (e.g., $u = 0.25$). In such a case, the effect of internal fluid flow can be expected to be insignificant. The frequency response diagrams shown in Fig. 6 will be analyzed in detail here.

In Fig. 6a, the excitation frequency is started at $\bar{\Omega} = 0$. As the excitation frequency is increased, the oscillation amplitude increases until a peak value is reached. This peak value of amplitude is around the first-mode resonant frequency ω_1 . From Table 1, it is noted that $\omega_1 \simeq 7.3456$. When the excitation frequency is further increased, the oscillation amplitude decreases first and then increases again, followed by an upward jump at a certain frequency slightly lower than the second-mode resonant frequency (as can be seen in Table 1, ω_2 is 26.7334 approximately). The frequency response diagram shown in Fig. 6a indicates that the jump phenomenon occurs at $\bar{\Omega} \approx 23.8$, with an accompanying increase in oscillation amplitude. After that jump point, the oscillation amplitude would decrease with increasing frequency.

If the excitation frequency is started at $\bar{\Omega} = 40$ and reduced, the results presented in Fig. 6b show that the oscillation amplitude increases until a peak value is reached at a certain frequency slightly lower than the second-mode resonant frequency. In Fig. 6b, the corresponding peak value of oscillation amplitude takes place at $\bar{\Omega} = 20.4$ approximately, which is much lower than the frequency value for peak amplitude shown in Fig. 6a. As the excitation frequency is decreased further, a downward jump takes place with an accompanying decrease in the oscillation amplitude, after which the oscillation amplitude decreases slowly first and then increases with decreasing $\bar{\Omega}$, followed by the occurrence of a peak amplitude response around the first-mode resonant frequency. As can be expected, after the peak amplitude response near ω_1 , the oscillation amplitude of the pipe would decrease with reduced excitation frequency.

From Fig. 6, the jump phenomenon associated with the second mode is clearly seen. Nevertheless, the frequency response curve near the first mode does not contain any obvious jumps. It is also noted that the amplitude curve near the first-mode resonant frequency almost remains neutral without bending to the left or the right. The nonlinearity in the pipe system, however, can bend the frequency response curve near the second-mode resonant frequency to the left, displaying a softening-type nonlinear behavior. Therefore, some of the responses near the second-mode resonant frequency are multivalued, while others are single-valued.

Shown in Fig. 8 are the phase portraits for the tip-end responses of the pipe and the shapes of the oscillating pipe for several typical values of excitation frequency, for the system defined in Fig. 6. When plotting the shapes of the oscillating pipe, the instantaneous shapes with the tip-end displacement reaching the maximum amplitude are highlighted in blue, while a certain instantaneous shape for the pipe with a moderate displacement is highlighted in red. It is observed from the phase portraits that, in all cases, the pipe undergoes a periodic motion, although the oscillation amplitudes are quite different for different excitation frequencies.

In the case of $\bar{\Omega} = 5$, since the excitation frequency is much smaller than the first-mode resonant frequency, the pipe has relatively small amplitude and undergoes mainly the first-beam-mode oscillations (Fig. 8a), with no higher-order beam-mode component. In the case of primary resonance near the first-mode resonant frequency, the oscillation amplitude becomes larger. The results for the shapes of the oscillating pipe shown in Fig. 8b indicate that the pipe still undergoes mainly the first-beam-mode oscillations for $\bar{\Omega} = 7.4$. It is noted that, for a certain moment, at which the maximum positive (or negative) displacement of the tip-end of the pipe is reached, the clamped end of the pipe is located at a negative (or positive) position, which is different from that shown in Fig. 8a. From the various shapes of the oscillating pipe, therefore, it seems that a fixed node exists near the clamped end of the pipe.

Shown in Fig. 8c is the response of the pipe far away from the first-mode resonant frequency, but near the second-mode one. By referring to Fig. 6a, it is easily understood that the oscillation amplitude for $\bar{\Omega} = 20$ is much smaller than that shown in Fig. 8b. By inspecting the shapes of the oscillating pipe,

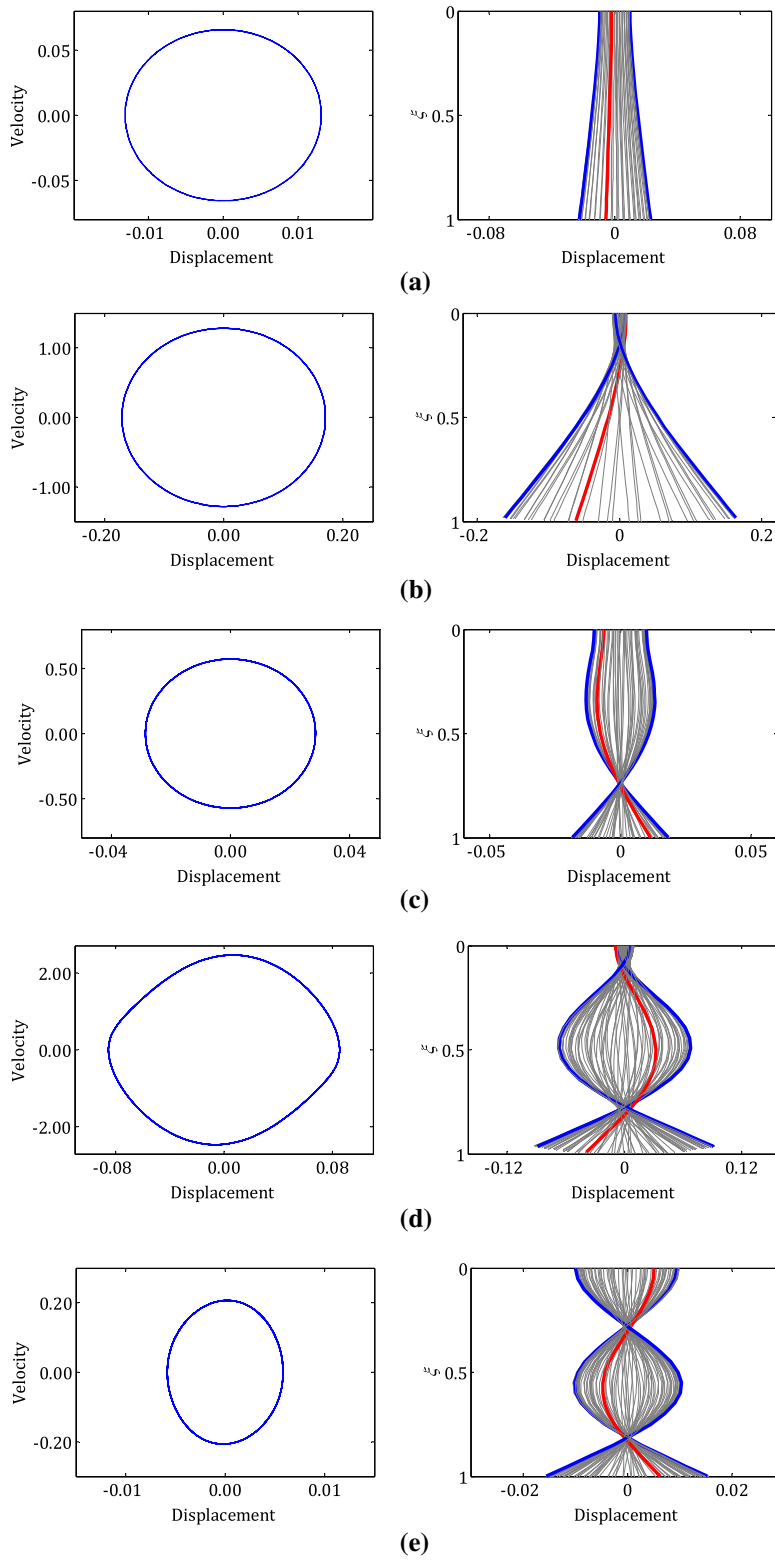


Fig. 8. Some phase portraits of the tip-end responses of the pipe defined in Fig. 6 and the shapes of the oscillating pipe for several typical values of excitation frequency; for each excitation frequency, the phase portrait is plotted on the left, while the shapes of the oscillating pipe are illustrated on the right; a $\bar{\Omega} = 5$, b $\bar{\Omega} = 7.4$, c $\bar{\Omega} = 20$, d $\bar{\Omega} = 24.25$, and e $\bar{\Omega} = 35$

it is figured out that the oscillations mainly contain the second-beam-mode component. Compared with that shown in Fig. 8b, the single fixed node in Fig. 8c is closer to the tip end of the pipe.

Interesting dynamic responses are obtained for $\bar{\Omega} = 24.25$, as shown in Fig. 8d. For such an excitation frequency near the second-mode resonant frequency, the pipe has a relatively large oscillation amplitude. It is clear that the shapes of the oscillating pipe mainly contain the second-beam-mode component. In this case, interestingly, the shapes of the oscillating pipe exhibit two fixed nodes: one near the clamped end and the other near the tip end.

The results shown in Fig. 8e are for a much larger excitation frequency (i.e., $\bar{\Omega} = 35$), which is far away from the second-mode and third-mode resonant frequencies. Thus, it is expected that the oscillation amplitude of the pipe would be small. From the shapes of the oscillating pipe, it is observed that two fixed nodes still exist and the upper node is away from the clamped end, which is different from that shown in Fig. 8d. Once again, it is seen that the shapes of the pipe mainly contain the second-beam-mode component.

From Figs. 6 and 8, therefore, an insight into the primary resonances associated with the first- and second-mode resonant frequencies has been obtained for $u = 0.25$. The pipe would be subjected to a periodic motion for all excitation frequencies in the domain of $[0, 40]$. As an important note, it should be mentioned that the excitation frequency has a significant effect on the shape of the oscillating pipe.

3.2.3. The Effect of Flow Velocity

The motivation for investigating the effect of internal flow velocity on the forced vibrations of the system mainly comes from two sources. The first is to obtain quantitative results for comparison against those for a pipe with extremely low flow velocities (e.g., $u = 0.25$). As mentioned in the foregoing, in the case of $u = 0.25$, the pipe may be approximately considered as an ‘empty’ beam. The second source of impetus was inspired from the Argand diagram shown in Fig. 3, where it is noted that the flow velocity has an important influence on the damping ratio of the system. Since the damping ratio for each mode strongly depends on the flow velocity, it is of interest to discover whether the pipe’s primary response near the first- or second-mode resonant frequency can be suppressed in the presence of internal fluid flow.

Extensive calculations of frequency response diagrams for several low/moderate values of flow velocity are conducted first. The flow velocities are selected to be below the critical value for flutter instability. A summary of the results is presented in Figs. 9, 10, 11, and 12.

As shown in Fig. 9, the two frequency response curves for $u = 1.0$ are closely similar to those plotted in Fig. 6. The jump phenomena near the second-mode resonant frequency are clearly observed. However, the most different feature between the results of Figs. 6 and 9 is that the peak amplitude related to the primary resonance near ω_1 for $u = 1$ is smaller than that for $u = 0.25$. The results shown in Fig. 10 indicate that the peak amplitude near ω_1 is further decreased when the flow velocity is set to be $u = 2$. Moreover, the jump phenomenon near the second-mode resonant frequency disappears, for the excitation frequency being varied either up or down through the frequency domain of $[0, 40]$. Thus, the frequency response curves for excitation frequency being varied up and down are identical.

More interesting dynamical behavior is obtained as the flow velocity is further increased. In Figs. 11 and 12 are respectively shown the frequency response diagrams for $u = 7.4$ and 8.5 , with the latter slightly below the critical flow velocity ($u_{cr} = 8.54$). It is observed from Figs. 11 and 12 that the primary resonances near ω_1 are not visible, while the peak amplitude near ω_2 becomes larger.

With regard to the foregoing discussion on the primary resonance near ω_1 , a very important point should be stressed. When the flow velocity is increased but below the critical value for flutter instability, the primary resonance near ω_1 diminishes. The underlying reason for this may be associated with the evolution of damping in the first mode with increasing flow velocity. By referring to Fig. 2, it is recalled that the damping ratio in the first mode becomes larger and larger as the flow velocity is increased. Accordingly, the primary resonance near ω_1 is damped and invisible eventually, highlighting the significant effect of flow velocity on the forced vibration behavior of the cantilevered pipe conveying fluid.

Next, we consider the effect of flow velocity on the dynamic responses of the pipe in the case that the flow velocity is so high that the pipe becomes unstable via flutter. The result shown in Fig. 13 is the frequency response curve for $u = 8.6$, which is just slightly higher than the critical value ($u_{cr} = 8.54$).

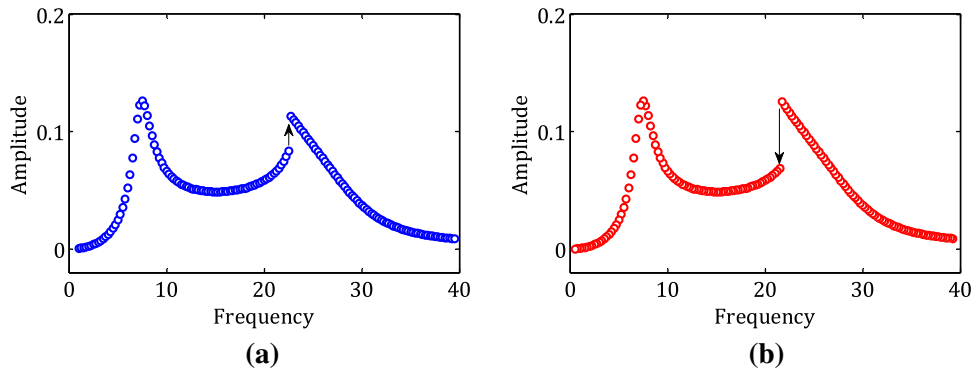


Fig. 9. Frequency response curves in the sense of primary resonances calculated using a four-mode approximation, for $u = 1.0$, $\mu = 0.02$, $\gamma = 26.75$, and $\beta = 0.213$; **a** the results for excitation frequencies being increased, and **b** the results for excitation frequencies being decreased

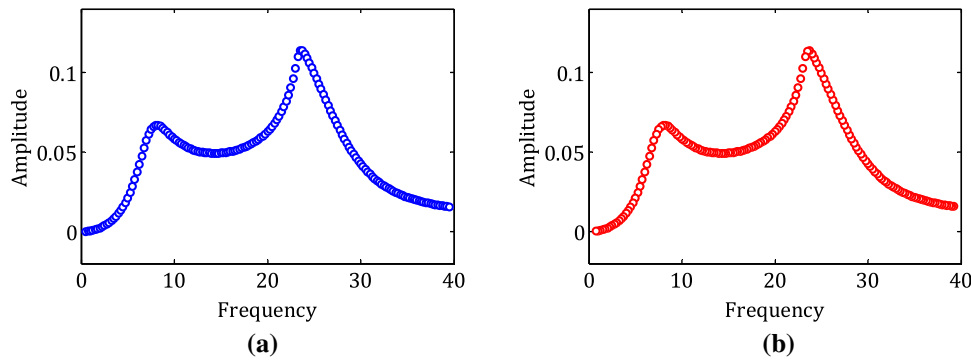


Fig. 10. Frequency response curves in the sense of primary resonances calculated using a four-mode approximation, for $u = 2.0$, $\mu = 0.02$, $\gamma = 26.75$, and $\beta = 0.213$; **a** the results for excitation frequencies being increased, and **b** the results for excitation frequencies being decreased

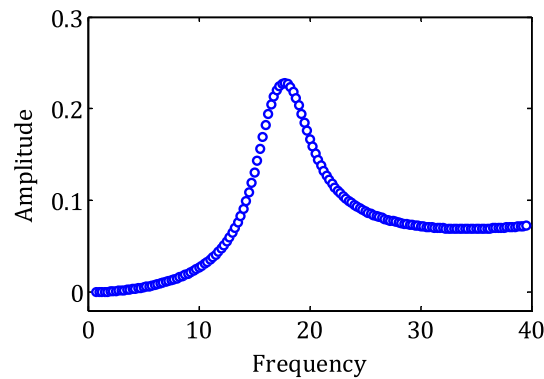


Fig. 11. Frequency response curves in the sense of primary resonances calculated using a four-mode approximation, for $u = 7.4$, $\mu = 0.02$, $\gamma = 26.75$, and $\beta = 0.213$

Since the flow velocity is beyond the flutter threshold, the pipe is concurrently subjected to flow-induced and forced vibrations. One might have thought that the dynamic response for $u = 8.6$ would significantly differ from that for $u = 8.5$. The difference between the results of frequency response diagrams shown in Figs. 12 and 13 does not seem to be pronounced. This is not the fact, however. It is essentially noted that, at about $\bar{\Omega} = 14.5$, there exists an unnoticeable valley on the frequency response curve, as can be seen in Fig. 13. The occurrence of the valley is somehow like the quenching

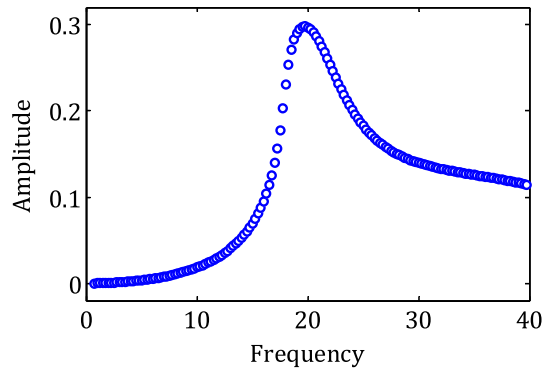


Fig. 12. Frequency response curves in the sense of primary resonances calculated using a four-mode approximation, for $u = 8.5$, $\mu = 0.02$, $\gamma = 26.75$, and $\beta = 0.213$

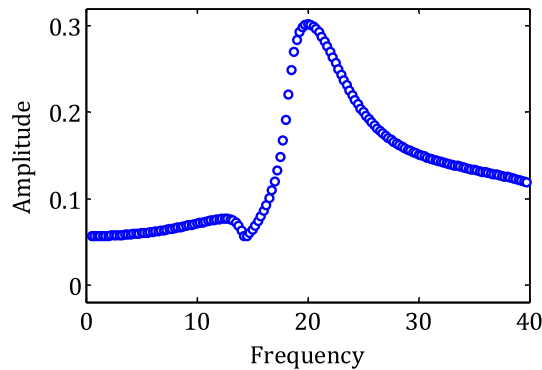


Fig. 13. Frequency response curves in the sense of primary resonances calculated using a four-mode approximation, for $u = 8.6$, $\mu = 0.02$, $\gamma = 26.75$, and $\beta = 0.213$

phenomenon [23]. In the following discussion, for convenience, the excitation frequency at which the valley occurs is termed as ‘critical excitation frequency,’ which shall be denoted by $\bar{\Omega}_{cr}$. The occurrence of the valley may be related to the possible dynamical behavior shown in Fig. 14, where some phase portraits and oscillating shapes for several excitation frequencies are plotted.

In Fig. 14a, b, both excitation frequencies are smaller than $\bar{\Omega}_{cr} \approx 14.5$. It is found that the pipe undergoes a non-periodic motion, which is more like a quasiperiodic motion. Indeed, when the excitation frequency is smaller than 14.5, the pipe is always subjected to this type of non-periodic motion. It is also seen that the shapes of the oscillating pipe mainly contain both the first- and second-beam-mode components. The results shown in Fig. 14c–f are presented for excitation frequencies larger than the critical value, $\bar{\Omega}_{cr} \approx 14.5$. Interestingly, it is seen in Fig. 14c–f that all the oscillations are periodic, which are different from those shown in Fig. 14a, b. Noting that with increasing excitation frequency, some of the oscillating shapes may contain the third-mode-beam component (Fig. 14e, f).

For a pipe with flow velocity beyond the critical value, therefore, it is found that the oscillation type of the pipe is strongly dependent on the excitation frequency. When the excitation frequency is smaller than the critical value ($\bar{\Omega}_{cr}$), the pipe undergoes quasiperiodic motions. In the case of excitation frequency being larger than $\bar{\Omega}_{cr}$, however, a limit cycle motion would be the preferred form of oscillations.

Similar results are shown in Fig. 15 in the form of frequency response diagram, for a slightly higher flow velocity of $u = 9$. In this figure, it is noted that the valley on the frequency response curve is more visible. In this case, the critical excitation frequency for the valley is found to be $\bar{\Omega}_{cr} \approx 19.2$. Compared with that shown in Fig. 14, the valley for $u = 9$ seems much narrower and is closer to the frequency for peak amplitude. Again, numerical calculations indicate that the pipe undergoes quasiperiodic motions

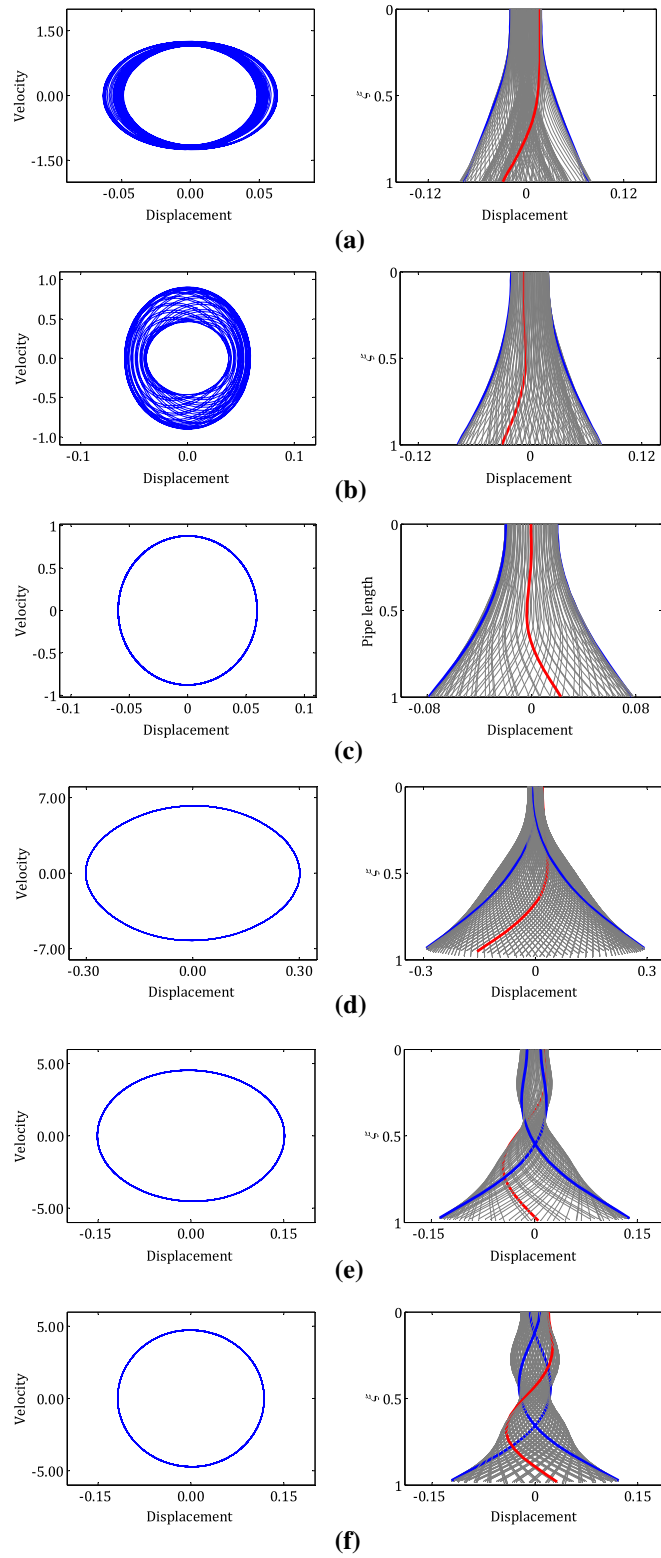


Fig. 14. Some phase portraits of the tip-end responses of the pipe defined in Fig. 13 and the shapes of the oscillating pipe for several typical values of excitation frequency; for each excitation frequency, the phase portrait is plotted on the left, while the shapes of the oscillating pipe are illustrated on the right; a $\bar{\Omega} = 7$, b $\bar{\Omega} = 14$, c $\bar{\Omega} = 14.75$, d $\bar{\Omega} = 20$, e $\bar{\Omega} = 30$, and f $\bar{\Omega} = 40$

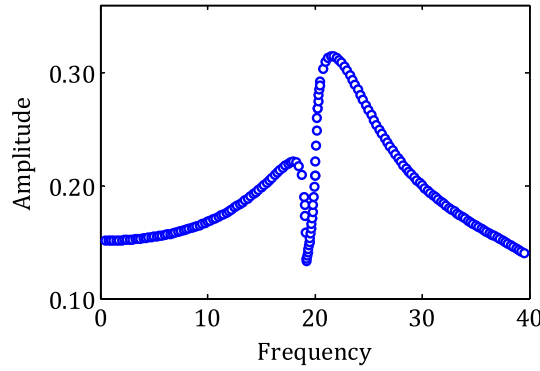


Fig. 15. Frequency response curves in the sense of primary resonances calculated using a four-mode approximation, for $u = 9.0$, $\mu = 0.02$, $\gamma = 26.75$, and $\beta = 0.213$

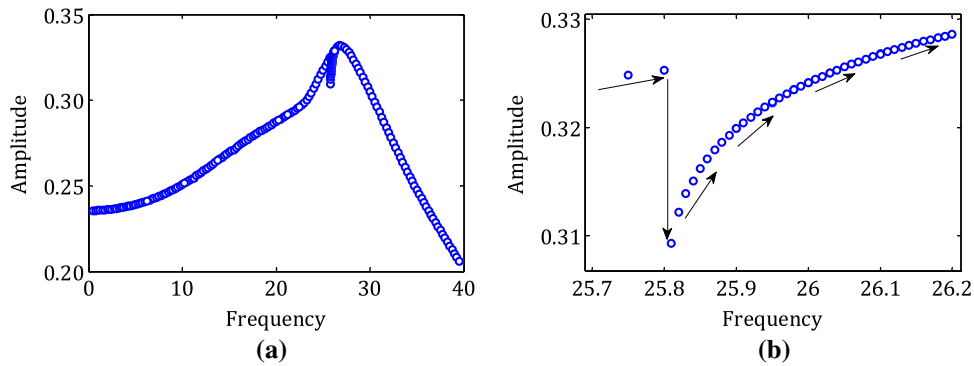


Fig. 16. Frequency response curves in the sense of primary resonances calculated using a four-mode approximation, for $u = 10.0$, $\mu = 0.02$, $\gamma = 26.75$, and $\beta = 0.213$, with the excitation frequency being varied **a** in the range of $0 \leq \bar{\Omega} \leq 40$ and **b** in a smaller range of $25.7 \leq \bar{\Omega} \leq 26.2$

for excitation frequencies smaller than $\bar{\Omega}_{cr} \approx 19.2$ and is subjected to a limit cycle motion for excitation frequencies beyond this critical value.

The final case to be considered is the pipe system with sufficiently high flow velocity (e.g., $u = 10$). In this case, the results shown in Fig. 16a indicate that the response of the pipe has a much larger amplitude for each excitation frequency. This is clear if a comparison is made between the results shown in Figs. 15 and 16. The increase in oscillation amplitude at each excitation frequency is due to the enhanced destabilization effect of internal fluid with increasing flow velocity. In Fig. 16a, it is also noted that the critical excitation frequency at the valley is much closer to the frequency value for the peak amplitude of the pipe. In the case of $u = 10$, it is observed from Fig. 16b that the critical excitation frequency is equal to $\bar{\Omega}_{cr} = 25.81$ approximately.

3.2.4. The Possibility of Superharmonic Resonances

In Sect. 3.2.2, the dynamic responses in the sense of primary resonances have been investigated with a small excitation amplitude of $\mu = 0.02$. When the excitation frequency is away from ω_i , the possible superharmonic and subharmonic resonances cannot be excited unless its amplitude is hard; that is, unless $\mu = O(1)$. By referring to Eq. (5), it is noted that the dynamical system is of cubic nonlinearity. Thus, the subharmonic resonance with $\bar{\Omega} \approx 3\omega_i$ and superharmonic resonance with $\bar{\Omega} \approx \omega_i/3$ may be possible. Since the excitation frequency of this study is limited to the domain $[0, 40]$, several attempts have been made for investigating the possible superharmonic or subharmonic resonances in the case of $\bar{\Omega} \approx \omega_1/3$, $\omega_2/3$ or $3\omega_1$. However, only the case of $\bar{\Omega} \approx \omega_1/3$ makes physical sense and will be considered in the following analysis.

Figure 17 is the summary of the results of superharmonic resonances with $\bar{\Omega} \approx \omega_1/3$ for $u = 0.25$ and various excitation amplitudes. Two interesting observations may be made: (i) the superharmonic

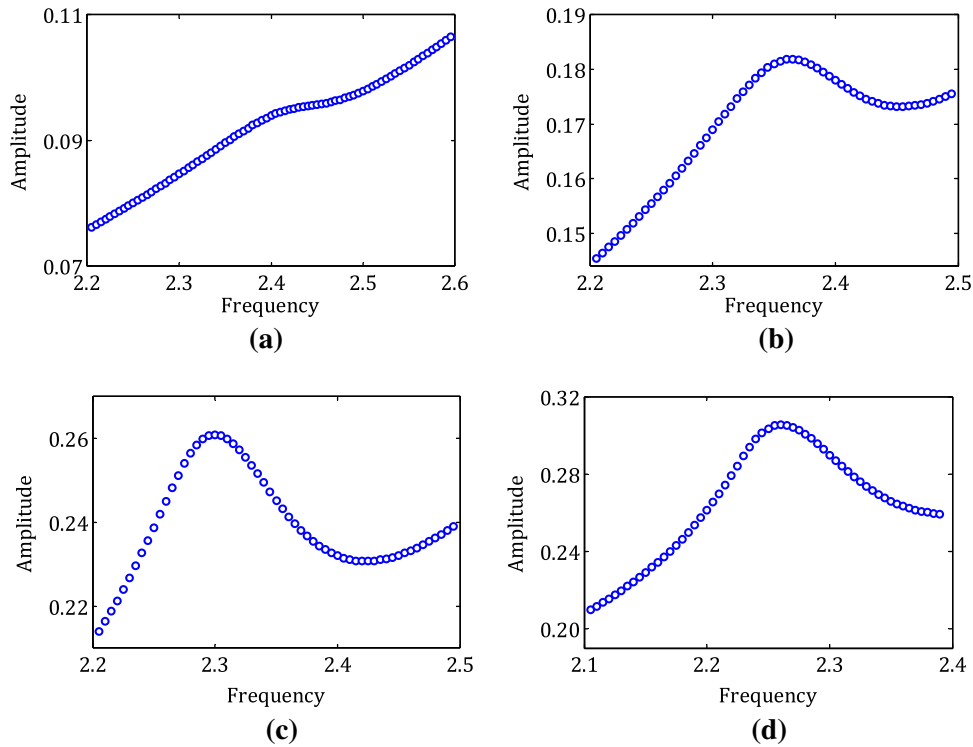


Fig. 17. Frequency response curves in the sense of superharmonic resonances calculated using a four-mode approximation, for $u = 0.25$, $\gamma = 26.75$ and $\beta = 0.213$, for several values of excitation amplitude; **a** $\mu = 0.5$, **b** $\mu = 0.9$, **c** $\mu = 1.2$, and **d** $\mu = 1.35$

resonance can be excited only for relatively large excitation amplitude (the superharmonic response shown in Fig. 17a for $\mu = 0.5$ is not pronounced); (ii) the excitation frequency at which the peak amplitude occurs may decrease with varying μ (e.g., for $\mu = 0.9$, 1.2, and 1.35, the excitation frequency for the peak amplitude is found to be 2.365, 2.3, and 2.26, respectively).

Further calculations have produced several phase portraits of the tip-end displacement of the pipe and the corresponding shapes of the oscillating pipe for $\mu = 1.2$ and three different values of excitation frequency. The results are shown in Fig. 18, from which it is seen that the shapes of the oscillating pipe are associated with the first-beam-mode component. In the case of $\bar{\Omega} = 2.3$, the phase portrait of Fig. 18b indicates that the pipe is subjected to a periodic motion, which is obviously different from the period-1 motion plotted in Fig. 18a, c. Therefore, the phase portrait for $\bar{\Omega} = 2.3$ clearly demonstrates the existence of superharmonic resonance in such a pipe system.

3.3. Discussion

In the present study, the cantilevered pipe is restricted to planar motions by embedding a thin metal plate all along its length. In such a case, the pipe always undergoes 2D periodic or quasiperiodic motions. If the thin metal plate is absent, however, kaleidoscopic non-planar responses are possible for some values of mass ratio, excitation frequency, and excitation amplitude, as pointed out in Ref. [33]. Indeed, 2D/3D chaotic motions, 2D/3D quasiperiodic motions, and 2D/3D periodic motions may occur. The mechanism of these complicated dynamical behaviors and their switch are still not well understood [3]. In this work, the motions of the pipe are restricted to a plane, which enables us to explore and understand the basic mechanism of fluid-conveying cantilevers undergoing both self-excited and forced vibrations.

In all the calculations, the mass ratio and gravity parameter are selected as $\beta = 0.213$ and $\gamma = 26.75$, which are the same as those in the experiment of Paidoussis and Semler [24]. For such a specific pipe system with $\beta = 0.213$ and $\gamma = 26.75$, chaotic motions have not been detected. However, this does not mean that chaos is impossible for some other values of μ , $\bar{\Omega}$, β , and γ . The existence of chaotic

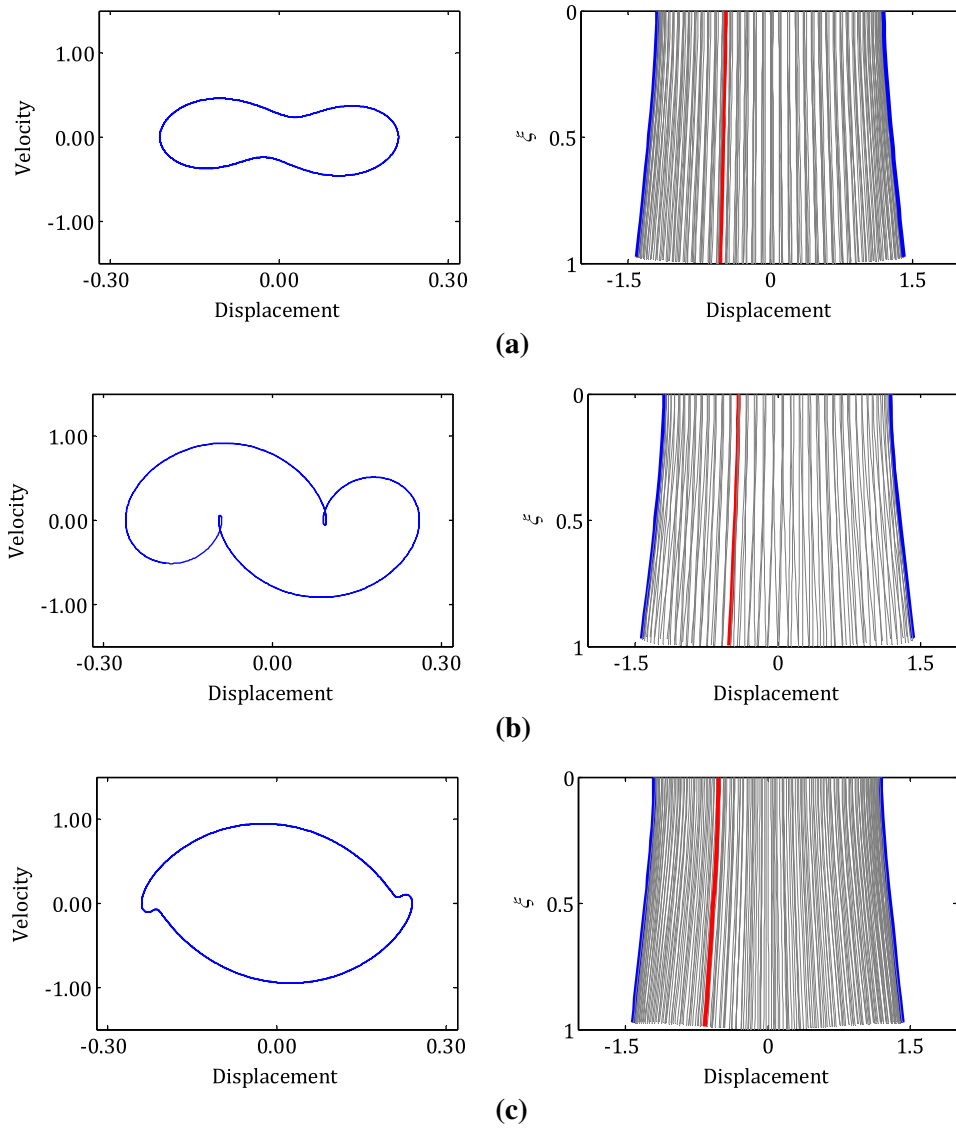


Fig. 18. Some phase portraits of the tip-end responses of the pipe and the shapes of the oscillating pipe for several typical values of excitation frequency ($u = 0.25$, $\mu = 1.2$, $\gamma = 26.75$, and $\beta = 0.213$); for each excitation frequency, the phase portrait is plotted on the left, while the shapes of the oscillating pipe are illustrated on the right; **a** $\bar{\Omega} = 2.2$, **b** $\bar{\Omega} = 2.3$, and **c** $\bar{\Omega} = 2.5$

oscillations in such a 2D pipe system under base excitations, which is another interesting topic, needs to be investigated in the future.

4. Conclusions

The forced oscillations of a cantilevered pipe conveying fluid under base excitations are examined in this work, with particular attention on the possibility of primary and superharmonic resonances when the excitation amplitudes and frequencies are varied. The analytical model, after Galerkin discretization to four degree-of-freedom, exhibits interesting dynamical behaviors.

It is found that, for low flow velocity, both the first- and second-mode primary resonances can be observed when the excitation frequency is either increased or decreased successively. The frequency response curves near the second-mode resonant frequency may display a softening-type nonlinear behavior with jump phenomenon in the oscillation amplitude. For moderate flow velocity below the flutter threshold, however, the primary resonance near the first-mode resonance frequency is not visible

due to the increased positive damping resulted from the internal fluid flow. Interestingly, the jump phenomenon in the oscillation amplitude near the second-mode resonant frequency may disappear with increasing flow velocity. In the case of a pipe with high flow velocity beyond the flutter threshold, quenching-like phenomena would occur, i.e., there exists a valley on the frequency response curve at a critical excitation frequency. The pipe would undergo quasiperiodic motions when the excitation frequency is smaller than the critical value, while it is subjected to periodic motions if the excitation is large than this critical value. The case of a pipe with large excitation amplitude is also considered, showing that a superharmonic resonance with $\bar{\Omega} \approx \omega_1/3$ is possible in this system.

The results obtained in this work highlight the dramatic role of internal fluid flow on the forced oscillations of cantilevered pipes conveying fluid.

Acknowledgements. This work is supported by the National Natural Science Foundation of China (Nos. 11622216 and 51409134).

References

- [1] Paidoussis MP. The canonical problem of the fluid-conveying pipe and radiation of the knowledge gained to other dynamics problems across applied mechanics. *J Sound Vib.* 2008;310:462–92.
- [2] Paidoussis MP, Li GX. Pipes conveying fluid: a model dynamical problem. *J Fluids Struct.* 1993;7:137–204.
- [3] Paidoussis MP. Fluid-structure interactions: slender structures and axial flow, vol. 1. 2nd ed. New York: Elsevier; 2014.
- [4] Wang L, Hong YZ, Dai HL, Ni Q. Natural frequency and stability tuning of cantilevered CNTs conveying fluid in magnetic field. *Acta Mech Solida Sin.* 2016;29:567–76.
- [5] He F, Dai HL, Huang ZH, Wang L. Nonlinear dynamics of a fluid-conveying pipe under the combined action of cross-flow and top-end excitations. *Appl Ocean Res.* 2017;62:199–209.
- [6] Dai HL, Wang L, Abdelkeri A, Ni Q. On nonlinear behavior and buckling of fluid-transporting nanotubes. *Int J Eng Sci.* 2015;87:13–22.
- [7] Yang TZ, Yang XD, Li YH, Fang B. Passive and adaptive vibration suppression of pipes conveying fluid with variable velocity. *J Vib Control.* 2014;20:1293–300.
- [8] Chen LQ, Zhang YL, Zhang GC, Ding H. Evolution of the double-jumping in pipes conveying fluid flowing at the supercritical speed. *Int J Non-Linear Mech.* 2014;58:11–21.
- [9] Modarres-Sadeghi Y, Paidoussis MP. Nonlinear dynamics of extensible fluid-conveying pipes, supported at both ends. *J Fluids Struct.* 2009;25:535–43.
- [10] Holmes PJ. Pipes supported at both ends cannot flutter. *J Appl Mech.* 1978;45:619–22.
- [11] Hu K, Wang YK, Dai HL, Wang L, Qian Q. Nonlinear and chaotic vibrations of cantilevered micropipes conveying fluid based on modified couple stress theory. *Int J Eng Sci.* 2016;105:93–107.
- [12] Modarres-Sadeghi Y, Paidoussis MP, Semle C. Three-dimensional oscillations of a cantilever pipe conveying fluid. *Int J Non-Linear Mech.* 2008;43:18–25.
- [13] Bajaj AK, Sethna PR. Flow induced bifurcations to three-dimensional oscillatory motions in continuous tubes. *SIAM J Appl Math.* 1984;44:270–86.
- [14] Semler C. Nonlinear dynamics and chaos of pipes conveying fluid. M.Eng. Thesis, Faculty of Engineering, McGill University, Montreal, Québec, Canada 1991.
- [15] Li GX, Paidoussis MP. Stability, double degeneracy and chaos in cantilevered pipes conveying fluid. *Int J Non-Linear Mech.* 1994;29:83–107.
- [16] Paidoussis MP, Semler C. Nonlinear dynamics of a fluid-conveying cantilevered pipe with an intermediate spring support. *J Fluids Struct.* 1993;7:269–98.
- [17] Paidoussis MP, Moon FC. Nonlinear and chaotic fluidelastic vibrations of a flexible pipe conveying fluid. *J Fluids Struct.* 1988;2:567–91.
- [18] Paidoussis MP, Li GX, Moon FC. Chaotic oscillations of the autonomous system of a constrained pipe conveying fluid. *J Sound Vib.* 1989;135:1–19.
- [19] Paidoussis MP, Li GX, Rand RH. Chaotic motions of a constrained pipe conveying fluid: comparison between simulation, analysis and experiment. *J Appl Mech.* 1991;58:559–65.
- [20] Jin JD. Stability and chaotic motion of a restrained pipe conveying fluid. *J Sound Vib.* 1997;208:427–39.
- [21] Jin JD, Zou GS. Bifurcations and chaotic motions in the autonomous system of a restrained pipe conveying fluid. *J Sound Vib.* 2003;260:783–805.
- [22] Xu J, Huang YY. Bifurcations of a cantilevered pipe conveying steady fluid with a terminal nozzle. *Acta Mech Sin.* 2000;16:264–72.
- [23] Ni Q, Wang YK, Tang M, Luo YY, Yan H, Wang L. Nonlinear impacting oscillations of a fluid-conveying pipe subjected to distributed motion constraints. *Nonlinear Dyn.* 2015;81:893–906.

- [24] Paidoussis MP, Semler C. Nonlinear and chaotic oscillations of a constrained cantilevered pipe conveying fluid: a full nonlinear analysis. *Nonlinear Dyn.* 1993;4:655–70.
- [25] Modarres-Sadeghi Y, Semler C, Wadham-Gagon M, Paidoussis MP. Dynamics of cantilevered pipes conveying fluid. Part 3: three-dimensional dynamics in the presence of an end-mass. *J Fluids Struct.* 2007;23:589–603.
- [26] Modarres-Sadeghi Y, Paidoussis MP. Chaotic oscillations of long pipes conveying fluid in the presence of a large end-mass. *Comput Struct.* 2013;122:192–201.
- [27] Yoshizawa M, Suzuki T, Takayanagi M, Hashimoto K. Nonlinear lateral vibration of a vertical fluid-conveying pipe with an end mass. *JSME Int J Ser C.* 1988;41:144–53.
- [28] Copeland GS, Moon FC. Chaotic flow-induced vibration of a flexible tube with end mass. *J Fluids Struct.* 1992;6:705–18.
- [29] Semler C, Paidoussis MP. Nonlinear analysis of the parametric resonances of a planar fluid-conveying cantilevered pipe. *J Fluids Struct.* 1996;10:787–825.
- [30] Folley CN, Bajaj AK. Spatial nonlinear dynamics near principal parametric resonance for a fluid-conveying cantilever pipe. *J Fluids Struct.* 2005;21:459–84.
- [31] Ilgamov MA, Tang DM, Dowell EH. Flutter and forced response of a cantilevered pipe: the influence of internal pressure and nozzle discharge. *J Fluids Struct.* 1994;8:139–56.
- [32] Furuya H, Yamashita K, Yabuno H. Nonlinear stability of a fluid-conveying cantilevered pipe with end mass in case of horizontal excitation at the upper end. In: *Proceedings FEDSM.* New York: ASME; 2010. p. 1219–1227.
- [33] Chang GH, Modarres-Sadeghi Y. Flow-induced oscillations of a cantilevered pipe conveying fluid with base excitation. *J Sound Vib.* 2014;333:4265–80.
- [34] Semler C, Li GX, Paidoussis MP. The nonlinear equations of motion of pipes conveying fluid. *J Sound Vib.* 1994;169:577–99.
- [35] Dai HL, Abdelkefi A, Wang L. Piezoelectric energy harvesting from concurrent vortex-induced vibrations and base excitations. *Nonlinear Dyn.* 2014;77:967–81.